Heliyon 6 (2020) e04179

Contents lists available at ScienceDirect

Heliyon

journal homepage: www.cell.com/heliyon

Research article

Impact of the drilling fluid system on the effectiveness of a high pressure jetting assisted rotary drilling system

Timon Echt [a], Thomas Stoxreiter [b], Johann Plank [a,*]

[a] Construction Chemistry, Department of Chemistry, Technische Universität München, Lichtenbergstr. 4, 85747 Garching, Germany
[b] Subsurface Engineering, Montanuniversitaet Leoben, Erzherzog Johann Straße 3, 8700 Leoben, Austria

ARTICLE INFO

Keywords:
Inorganic chemistry
Mechanical engineering
Geothermal energy
Drilling
Enhanced drilling technology
High pressure jet assisted rotary drilling
Water based drilling fluids
Sepiolite clay
Crystalline rock

ABSTRACT

An enhanced drill bit combining high pressure fluid jetting with a conventional rotary drilling system incorporating a tailored drilling fluid was designed to improve drilling performance in hard crystalline rock. Full scale drilling experiments (8 ½ inch bit size) were performed utilizing a specially designed sepiolite fluid and comparing its performance with water and xanthan gum as a standard geothermal drilling fluid. The novel drilling system improved the rate of penetration by over 70% compared to the conventional drill bit without jetting assistance. In addition, the sepiolite drilling fluid retained its fluid properties even after high pressure jetting.

1. Introduction

In order for EU member states to achieve their goals of reduced CO_2 emissions, renewable energy is a key component. Deep geothermal energy is a continuous and dependable electricity and heat source. However, due to the large depths and the prevalence of crystalline rock formations, drilling expenditures often constitute more than 50 % of total geothermal project costs. Therefore, enhancing drilling rates can significantly reduce costs and increase the economic viability of deep geothermal projects. The EU research project "ThermoDrill" therefore is developing an improved and revised drilling system to improve rate of penetration. It aims to achieve this by combining a high pressure jetting with conventional rotary drilling while utilizing an optimized drilling fluid as a combined drilling and jetting fluid.

One possibility to improve ROP and thus reduce drilling costs is to use drilling fluids with enhanced carrying capacity allowing for better cuttings removal from the borehole, thus leading to faster drilling (Becker et al., 1991; Robinson and Morgan, 2004). If the carrying capacity of a fluid is too low, then a significant amount of drilling energy is spent on finely regrinding the cuttings which reduces ROP. If the carrying capacity is high, then the cuttings can be removed faster and more efficiently increasing ROP. To achieve this, a fluid must possess sufficient viscosity at low shear rates to be able suspend the cuttings. However, at the same time the fluid must exhibit low viscosity at high shear rates in order to flow into the rock fractures induced by the drill bit. Consequently, the hydrostatic overbalance pressure exerted on the rock cuttings, which presses the cuttings against the formation, is reduced allowing for easier removal (Mansell and Haughs, 2018). At the high temperatures routinely encountered during deep geothermal drilling, this problem is even more severe as many fluids exhibit strong thermal thinning which significantly reduces their suspending properties and thus the ROP.

Therefore, the use of optimized fluids with thickening agents suited to the expected conditions, providing sufficient viscosity to suspend cuttings even at high temperatures, is highly beneficial (Caenn and Chillingar, 1996; Wise et al., 2010). For this reason, sepiolite, a clay known for its temperature stability, was chosen as a viscosifying agent. It is a natural phyllosilicate and is represented by the general chemical formula $Si_{12}Mg_8O_{30}(OH)_6(OH_2)_4 \cdot 8H_2O$. It forms small needle like particles with varying size which when properly dispersed in water can aggregate and associate to form a random edge-to-face network. The needles generally possess a thickness of ~20 nm and a length of up to 2 μm though this can vary depending on the geological origin of the sample. This network is highly shear thinning while simultaneously possessing excellent suspending properties even at high temperature. Hence, it has previously been evaluated as a candidate for high temperature geothermal wells (Zilch et al., 1991; Altun et al., 2015). Sepiolite of sedimentary origin

* Corresponding author.
E-mail address: sekretariat@bauchemie.ch.tum.de (J. Plank).

https://doi.org/10.1016/j.heliyon.2020.e04179
Received 28 January 2020; Received in revised form 27 March 2020; Accepted 5 June 2020

Table 1. Capabilities of the drilling test bench.

Property	Maximum capability
Weight on bit	25 tons
Rotations per minute	1000 rpm
Torque	500 dNm
Overburden pressure	70 MPa
Confining pressure	50 MPa
Drilling length	480 mm

containing smaller fibers is considered safe for use in drilling activities (IARC, 1997).

As a reference system, xanthan gum was chosen as it is commonly used as a thickening agent when drilling geothermal wells in Europe and thus presents state of the art. Xanthan gum is a water-soluble polysaccharide biopolymer which possesses high low shear rate viscosity under ambient conditions though it degrades at elevated temperatures and thus loses carrying capacity downhole. In general, only water based mud systems were considered for obvious reasons concerning the application in geothermal drilling projects.

Another option to enhance drilling rates in crystalline rock is to improve the drill bit by combining conventional rotary drilling with hydraulic high pressure jetting, as for instance hydraulic water cutting is used to great effect to cut granite blocks in quarries (Reichman, 1977; Kolle, 1987; Stoxreiter et al., 2018). The basic concept is to have a high velocity fluid jet exiting through nozzles at the edge of the drill bit thus cutting an annular groove therefore making the conventional drilling in the center easier and faster.

In order to achieve sufficient cutting depths, a high velocity fluid jet is required thus necessitating high pressures (usually >1,000 bar for hard rocks). However, not only the pressure but also the hydraulic power and the stand-off distance are critical parameters for an adequate cutting performance downhole. As generating the pressure at the surface is a significant safety hazard and the large distances lead to significant pressure losses in the fluid stream (Maurer et al., 1973), the concept of hydraulically driven down hole pumps was developed (Veenhuizen et al., 1996).

The goal of this work was to evaluate the influence of different combined drilling/jetting fluids on the ROP and performance of the enhanced drill bit combining high pressure fluid jetting with a conventional rotary drilling system as well as determining the influence of high pressure jetting on two different drilling fluids. Therefore, a sepiolite and a xanthan fluid possessing the same low shear rate values (3 rpm = 10 Lbf/100 ft^2, 6 rpm = 12 Lbf/100 ft^2) and density (1.1 g/mL) were prepared to allow a direct comparison. Fluid samples were taken from different locations in the test setup and the relevant drilling parameters (rate of penetration, weight on bit and mud pressure) were continuously monitored during the experiments. The tests were conducted at the drilling simulator test bench of the Mines Paris Tech (Pau, France) using tap water as a reference fluid system and a standard roller cone bit as a benchmark.

2. Experimental setup

2.1. Drilling simulator

In order to test the combined capabilities of the novel drilling fluid with the drill bit prototype, experiments were performed at the drilling simulator test bench of the Mines Paris Tech (Pau, France). Here, full-scale tests using an 8 ½ inch bit could be conducted under downhole representative conditions. The maximum capabilities of the drilling test bench are displayed in Table 1.

The rock sample to be drilled was placed in a pressure vessel which can simulate the desired pressures. Weight on bit (WOB) was controlled during testing and could be continuously adjusted as desired up to 20 tons while the drill bit could be rotated at up to 1,000 rpm. The drilling mud was fed into the system with a PL7 Gardner Denver pump while the mud pressure was increased with a controlled valve in the return pipe. WOB, torque as well as the different pressure types were measured throughout testing. Rate of penetration was determined continuously by measuring the derivation of the bit position.

In order to test the effectiveness of the high pressure jetting assisted drill bit, modifications and additions to the test bench were necessary (Stoxreiter et al., 2019). These were required in order to integrate the high pressure tubing. The required high pressure was provided by a mobile URACA Jet Power 300–1000 pump with a maximum flow rate of 55 Lpm at 2500 bar. Preliminary tests with an initial pressure of 2500 bar showed that pressure losses along the high pressure tubing are in the range of 150–300 bar. The high pressure swivel was equipped with a gap seal which had a slight leakage by design allowing the sampling of fluid after high pressure pumping but before jetting.

2.2. Preparation of drilling fluids

4500 L of a sepiolite and a xanthan gum fluid were prepared beforehand and shipped in intermediate bulk containers (IBCs) to the drilling simulator facility for the tests. The concentrations, given in % by weight of water (% bwow) of the thickening agents, were adjusted so that both fluids possessed the same low shear rate viscosity (3 rpm = 10, 6 rpm 12 Lbf/100 ft^2) and density (1.10 g/mL) after mixing to allow a meaningful comparison of both fluids.

The 1.65 wt.% sepiolite fluid was prepared using the recipe shown in Table 2. 23 kg of water were weighed into a 60 L barrel and the mixing head (type: G 65 M) of the Ultra Turrax T65 (IKA-Werke GmbH & Co. KG) was completely immersed in the water. The sodium carbonate (technical grade, from Novacarb) was predissolved within 2 min by mixing at 5000 rpm. The sepiolite (Berkbent Marine purchased from Tolsa SA) was added within 1 min while mixing at 8000 rpm and then mixed for further 8 min at 8500 rpm. The remaining 23 kg of water were added and mixed for 4 min at 8500 rpm, then the KCl (technical grade from Brenntag Polska Sp. z o.o) was added and mixed for another 4 min at 8500 rpm. The suspension was then homogenized for 10 min at 500 rpm with a propeller type mixer (EUROSTAR power control visc stirrer, IKA-Werke GmbH & Co. KG) before it was filled into the IBCs.

The xanthan gum drilling fluid was prepared by Sirius-ES Handels GmbH by first dissolving the sodium carbonate and potassium chloride before adding the xanthan gum (S-ES Bio XG, Sirius-ES Handels GmbH). The recipe is shown in Table 3.

Table 4 shows a direct comparison of the fresh fluid before testing. Both show similar values, though the sepiolite fluid is more shear

Table 2. Recipe of 1.65 wt.% sepiolite drilling fluid.

Component	Amount (kg)	Concentration % bwow
DI water	46.0	-
Sepiolite	0.76	1.65 %
Na_2CO_3	0.31	0.67 %
KCl	8.1	17.6 %

Table 3. Recipe of 0.53 wt.% xanthan gum drilling fluid.

Component	Amount (kg)	Concentration % bwow
Tap water	940 L	-
Xanthan gum	5.0	0.53 %
Na_2CO_3	2.0	0.21 %
KCl	176	18.7 %

Table 4. Comparison of the rheological properties of the fresh drilling fluids before testing.

Fluid	Shear stress (Lbf/100 ft^2)							
	600 rpm	300 rpm	200 rpm	100 rpm	6 rpm	3 rpm	Yield Point (YP)	Plastic Viscosity (PV)
Sepiolite	43	36	33	28	12	11	29	7
Xanthan gum	43	32	28	21	13	11	21	11

Table 5. Physical and mechanical properties of the Neuhauser granite.

Property	Value
Density (g/cm^3)	2.7
Porosity (%)	3.0 % (Diethart-Jauk and Gegenhuber, 2018)
Permeability (mD)	0.00–0.07 (Diethart-Jauk and Gegenhuber, 2018)
Young's modulus (GPa)	67 ± 7.8
Jetting threshold pressure (bar)	1000.0 (Stoxreiter et al., 2018)

thinning with a lower plastic viscosity and a higher yield point. The 3 and 6 rpm values of both fluids are slightly higher than desired but almost identical allowing for a meaningful comparison.

2.3. Drill bit

To evaluate the effectiveness of the jetting assisted drilling, two different bit types were evaluated in combination with the drilling fluids. A "8-1/2" "GF45Y" IADC 627Y roller cone bit with three cones served as the reference, as this bit type is commonly used to drill in deep granite. Two patent pending drill bit prototypes (IADC 627Y) were designed and manufactured during the project. These jetting assisted drill bits had an identical cutting structure with three cones with the same cutting element as the reference bit to allow a direct performance comparison. The prototypes possessed two separate conduits, one is an independent high pressure conduit which provides the fluid for the high pressure jetting nozzles while the low pressure conduits provided the normal drilling mud with sufficient flow rate to ensure proper hole cleaning by removal of the cuttings and fines.

The same hardened steel nozzles were used for all high pressure jetting assisted tests relevant for the present article. They had a diameter of 1.3 mm and a stand-off distance from nozzle outlet to rock surface of 6–8 mm. The discharge factor was 0.97 and they were provided by URACA GmbH & Co. KG.

2.4. Rock sample

Neuhauser granite was chosen as it is regarded to be representative of the crystalline rock types expected in deep geothermal wells in continental Europe. Additionally, Neuhauser granite is relatively homogenous, has appropriate hardness in terms of resistance against drilling and other rock desirable mechanical parameters (Table 5), so that representative results can be achieved. Its main mineral phases are feldspar, quartz and dark mica. The samples (diameter 310 m and height 380 mm) were extracted from a quarry in Upper Austria.

2.5. Testing procedure

The testing procedure was designed in order to determine the ability of high pressure jetting to influence ROP as well as the impact of the high pressure jetting on the drilling fluid properties. As earlier work had demonstrated that the overburden and confining pressure have a negligible impact on ROP, the confining and mud pressure were kept identical (100 bar) while the overburden pressure was set high enough (140–300 bar) to prevent the rock core from rotating with the drill bit (Garnier and van Lingen, 1958; Warren and Smith, 1985; Stoxreiter et al., 2019). The flow rate for the conventional mud supply was 600 Lpm with a constant injection pressure of approximately 110 bar, resulting in a mud pressure of 100 bar due the pressure losses around the drill bit. The different types of pressure were recorded continuously with pressure transducers. For the jetting assisted tests, the nozzle stand-off distance to the rock surface was 6–8 mm.

6 different test series were performed, 3 sets of tests using the conventional drill bit with the 3 separate fluid systems and 3 sets of tests with one prototype bit. Although additional experiments with the second bit prototype were performed, these are not considered relevant in the current article because only tap water was used as drilling fluid. The sole difference between the two bit prototypes was the number of high pressure nozzles and conventional nozzles. The different conditions are summarized in Table 6. Each test was performed twice, except in the case of the of drill bit prototype with xanthan gum as the rock sample broke during testing resulting in a mechanical failure of main parts of the test bench, therefore testing could not be continued.

The testing procedure remained identical for all tests except for the additional steps required for the high pressure jetting assisted experiments. After the granite sample was mounted, the overburden and the confining pressure were applied before the mud flow was initiated. The first 4 cm into the rock were drilled slowly to engage the bit properly, before testing was started, to ensure comparable conditions for all tests. In case of the jetting assisted tests, the lowest possible jetting pressure of approximately 1200 bar was applied during this first phase to ensure that particles did not enter the jetting nozzle and high pressure line and was subsequently increased to 2200 bar pressure at the drill bit. The rotational speed of the drill bit was set at 60 rpm, while the WOB was increased in set intervals (approximately 5 tons) from 5 to 15 tons during the measurement. Testing was stopped when the final drilling depth was reached after which the drilling mud flow and high pressure jetting supply were stopped simultaneously.

2.6. Drilling fluid sampling

Fluid samples were collected from different points of the drilling simulator test setup. Shown in Figure 1 is a general schematic of this setup. The blue line shows the jetting fluid side with three sampling points while the drilling mud side in orange was sample twice, at the start and end of the test.

Sample 1_{IBC}: This represents unused fresh fluid. The initial jetting fluid (sampling point **1_{IBC}**) was taken from an IBC containing pristine fluid (sepiolite and xanthan gum drilling fluids, **Nr 1** in Figure 1, blue line) or from a hose in the case of tap water. Prior to testing the sepiolite drilling fluid was mixed for 15 min using an adjustable stirrer (EZR 20 r, Elektrowerkzeuge GmbH Eibenstock, Eibenstock). Only fresh drilling fluid was supplied to the high pressure pump to avoid damage of the mechanical components by the cuttings and fines.

Sample $2_{HP\ Line}$: This sampling point shows just the impact of the high pressure pumping (2200 bar) as it is taken before jetting has occurred. The fluid was first pumped through a booster pump, then through the HP pump located in a truck stationed outside of the facility and then pumped at a rate of ~54 Lpm through a 8 mm diameter high pressure hose (length 30 m). The sample **$2_{HP\ Line}$** was taken from the runoff of the rotating seal.

Sample 3_{Nozzle}: This sample shows the additional influence of jetting on the high pressure pumped fluids. The fluid was jetted through a nozzle with an approximate velocity of 660 m/s and a pressure of 2200 bar (**Nr 3**

Table 6. Testing parameters.

Bit type	Drilling fluid	Pressure at bit (bar)	HP nozzle flow rate (Lpm)	HP nozzle diameter (mm)	HP hydraulic power (KW)
Standard	Water	-	-	-	-
	Sepiolite				
	Xanthan gum				
1-nozzle	Water	2200	54.1	1.3	198.4
	Sepiolite				
	Xanthan gum*				

* rock sample broke during test.

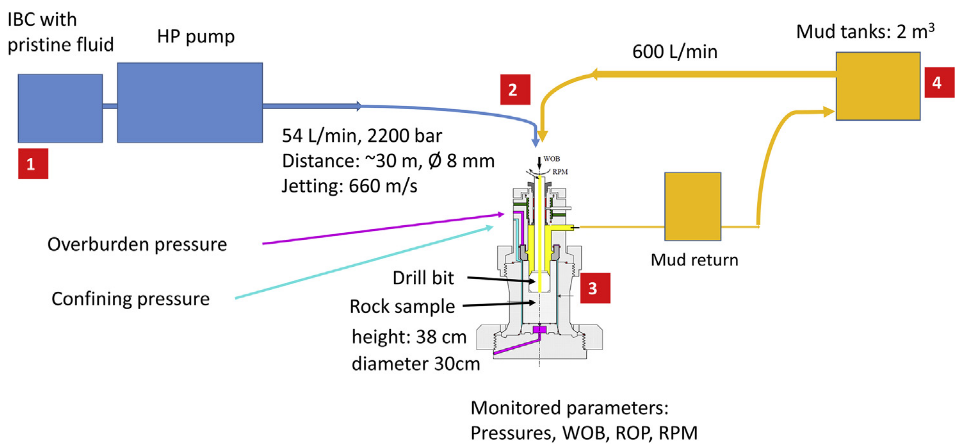

Figure 1. Schematic of fluid sampling points.

in Figure 1) where it becomes part of the drilling mud circuit (in orange). During normal testing, this fluid mixed with the drilling mud. Therefore, after a drilling/jetting test was concluded, the granite sample was removed and an old core placed inside. Then the fluid was jetted for a duration of 100 s at the same maximum pressure which was used during testing. This ensured that any fluid remaining in the test chamber was removed as over 70 L have subsequently been jetted into an old core. The jetting nozzle was located ~20 cm above the bottom of the granite core.

The drilling fluid was stored in a mud tank (**Nr. 4** in Figure 1) and circulated at a rate of 600 Lpm through the testing chamber and back to the mud tank (orange circuit).

Sample 4$_{\text{Mud-start}}$: This refers to the sample taken from the mud tank before the start of the test. In case of the sepiolite mud, the mud was mixed for 15 min with the propeller type mixer located in the tank to ensure the fluid was homogeneous. Samples were taken directly before testing started.

Sample 4$_{\text{Mud-end}}$: This sampling point refers to the sample taken from the mud tank after the drilling/jetting test was concluded and presents a mixture of the initial drilling mud together with jetted fluid and drill solids.

An overview of the test setup is shown in Figure 2 while Table 7 shows a short overview of the different sampling points.

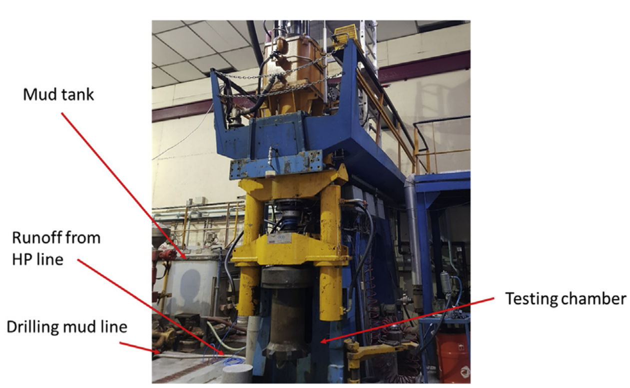

Figure 2. Testing setup.

2.7. Measurement of fluid properties

To determine the rheology of the drilling fluids, the testing procedure followed the guidelines set forth in API RP13B-1 (API, 2004). Mud weight was determined using a mud balance (Baroid Industrial Drilling Products). Fluid temperature was measured directly after sampling at the respective sampling point.

Fluid rheology was measured directly after sampling as well as after cooling to ambient (22 °C) by placing the fluid in measuring cup of the rheometer (Model 286 variable speed coaxial cylinder rheometer from Baroid Industrial Drilling Products). Dial readings were determined in 10 s intervals and the rotational speed was decreased according the pre-determined sequence (600–300–200–100 – 6–3 rpm). To obtain the shear stress values (Lbf/100 ft^2), the observed dial readings were multiplied with 1.066 due to the torsion spring factor of the rheometer (F = 1.0).

$$\text{PV (Lbf/100 ft}^2) = \theta(600) - \theta(300) \tag{1}$$

$$\text{YP (Lbf/100 ft}^2) = \theta(300) - \text{PV} \tag{2}$$

If a Bingham type flow behavior is assumed, the plastic viscosity (PV) can be calculated using Eq. (1) while the Yield Point (YP) can be determined using Eq. (2). θ(300) is the shear stress value (in Lbf/100 ft^2) of the fluid at 300 rpm. As the PV was calculated according to the API norm, the unit here is Lbf/100 ft^2 and not the usual Pa·s.

Furthermore, using linear regression, the parameters of the Bingham model (plastic viscosity (PV$_M$ in cp*s) and yield point (YP$_M$ in Lbf/100 ft^2)) as well as the parameters of the Power Law model (flow consistency index (K, Lbf/100 ft^2*s^n) and flow behavior index (n, dimensionless)) were calculated.

Table 7. Overview of sampling points.

Sampling point	Description
1_{IBC}	Pristine drilling fluid
$2_{HP\ Line}$	Fluid pumped at high pressure
3_{Nozzle}	Jetted fluid
$4_{Mud\text{-}start}$	Drilling fluid before start of test
$4_{Mud\text{-}end}$	Drilling fluid after test has concluded

3. Results and discussion

3.1. Testing with conventional drill bit

The rate of penetration was measured against increasing weight on bit using the conventional drill bit (Figure 3). The ROP was similar for tests with water and sepiolite and slightly lower for the tests with xanthan gum. The ROP increased linearly with increasing WOB for all systems. An enhanced ROP due to the better carrying capacity of the drilling fluids was not expected under these conditions as the maximum drilled depth into the sample was only 25 cm. This depth was too small to observe any significant benefits from the better suspending properties of the xanthan gum or sepiolite fluid as would be seen in the field when drilled depths can be upwards of 5 km. The reduced ROP could be due to a lower flowability, higher plastic viscosity, of the initial xanthan gum fluid compared with sepiolite, despite having the same low shear rate values, or water as more viscous fluids have a harder time flowing into the rock fractures induced by the drill bit. This reduces the hydrostatic overbalance pressure which presses the cuttings against the rock making them harder to remove (Mansell and Haughs, 2018).

3.2. Testing with 1 nozzle drill bit

As with the conventional drill bit, the rate of penetration was measured continuously throughout the testing of the jetting assisted drill bit. After an initial step in which the drill bit was brought into position and allowed to drill a set distance of 4 cm at a low jetting pressure, the actual test (~10 min) was started. The jet pressure was increased to maximum and the weight on bit increased continuously at set intervals. A quasi-static state was reached very quickly at the particular weight on bit levels and therefore allowed the reliable determination of the associated ROP. The average value of pressure reached at the bit was approximately 2200 bar. The ROP was plotted against the WOB (Figure 4) for all tests conducted except for the xanthan gum test as unfortunately no drilling data is available due to a mechanical problem with the drill string resulting from a broken rock sample. This did not have an impact on the fluid sample collection, however no ROP data are therefore available. The lines represent the average ROP from 2 tests. The maximum ROP was reached when jetting with 1 nozzle and water which was about 70 % higher compared to the baseline using a conventional drill bit with water demonstrating the effectiveness of the drill bit prototype.

With sepiolite, the ROP of the drill bit with 1 jetting nozzle was slightly lower than with water, though still much higher than the baseline using a conventional bit with water. The lower ROP observed for sepiolite at higher WOB was not directly related to the drilling process but was due to the continuous erosion of the jetting nozzle. The erosion led to a wider nozzle diameter and therefore a lower jetting pressure. However, the use of hard metal nozzles in later jetting tests with the fluid system reduced nozzle erosion to similar levels. No influence of the increased carrying capacity of the sepiolite fluid compared to that of water was to be expected, as the maximum drilling height of around 25 cm was too low for the higher carrying capacity to play a role.

Unfortunately, the experiment with xanthan gum could not be completed as the rock sample broke during testing resulting in a mechanical failure of main parts of the test bench. Therefore, the test with xanthan gum could not be performed.

The cutting action of the jetting could be visually observed in the granite samples. Shown in Figure 5 is a core drilled conventionally as well as a core drilled using the drill bit with 1 jetting nozzle and sepiolite as drilling/jetting fluid. A pronounced cut could be observed at the edge of the drilled area.

3.3. Drilling test – 1 jetting nozzle with sepiolite as drilling/jetting fluid

Sepiolite fluid samples were collected twice from all sampling points except for from the nozzle, which was sampled only once. The rheology, temperature at the source, temperature after rheology measurement as well as pH and density were determined directly after the samples were collected. A comparison of the Bingham and Power Law model parameters as calculated by linear regression and determined via Eqs. (1) and (2) respectively for the sepiolite drilling fluid measured directly after sample collection are shown in Table 8 while the rheology plot is shown in Figure 6. The model parameters and the rheology plot of the sepiolite fluid after it had cooled to ambient (22 °C) are displayed in Table 9 and Figure 7 respectively.

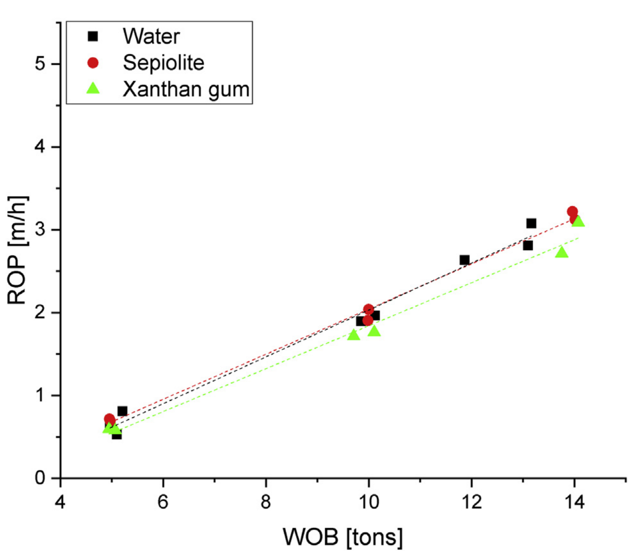

Figure 3. Rate of penetration for tests with a conventional drill bit.

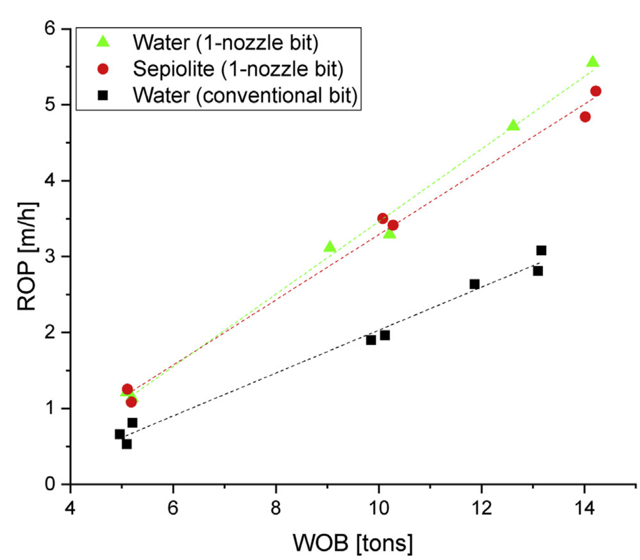

Figure 4. Rate of penetration for tests with the 1-nozzle bit and conventional bit.

Figure 5. Left: Core drilled conventionally, no jetting; Right: Core drilled using the 1-nozzle bit with sepiolite drilling fluid.

The fresh sepiolite fluid, 1_{IBC}, possessed excellent shear thinning properties, maintaining a high yield point and high low shear rate values (3 rpm value of 11 Lbf/100 ft^2) while also showing a low plastic viscosity. The same is true for the YP_M and PV_M calculated by linear regression and the flow behavior index (n) remains relatively constant at about 0.26 whereas the flow consistency index (K) stays constant at 8–9 Lbf/100 $ft^2{*}s^n$ when measured directly after sampling with slightly higher K values obtained after cooling. High pressure pumping increased the viscosity, especially the high shear rate values were higher (after cooling: 600 rpm = 54 Lbf/100 ft^2 compared with 43 Lbf/100 ft^2 initially). Generally, the sepiolite fluid samples did not possess a good fit with the Bingham model but showed an excellent fit with the Power Law model.

After passing through the nozzle, the high shear rate viscosity of the sepiolite fluid was reduced to its initial values when measured after cooling to ambient (600 rpm value: 41 Lbf/100 ft^2 compared with 43 Lbf/100 ft^2 initially) but lower than for the sample taken after high pressure pumping ($2_{HP\ Line}$). The low shear rate viscosity remained constant for all samples, except for $2_{HP\ Line}$ which was slightly higher.

Despite high pressure pumping and the very high velocity (~660 m/s) when passing through the nozzle, the sepiolite fluid remained mostly unchanged showing its high shear stability. The pH value and density of the sepiolite remained unchanged. The presence of fines in the fluid which circulated as drilling mud ($4_{Mud\text{-}end}$) was evident due to slight fluctuation of the shear rate values during the measurement due to bridging.

A slight optical change was observed for the sepiolite sample which had only been pressurized to 2200 bar and was pumped through the high pressure line as it was significantly darker than the sample from the IBC. The sample which had passed through the nozzle was somewhat darker, probably due to erosion of the high pressure tubing.

3.4. Drilling test – 1 jetting nozzle with xanthan gum as drilling/jetting fluid

As with sepiolite, xanthan gum fluid samples were collected from all sampling points for the only test which could be carried with the xanthan gum drilling fluid. Table 10 shows the model parameters for the xanthan gum fluid measured directly before and after testing, while Table 11 shows the values for the samples after they had cooled to 22 °C. The respective rheological plots are found in Figures 8 and 9.

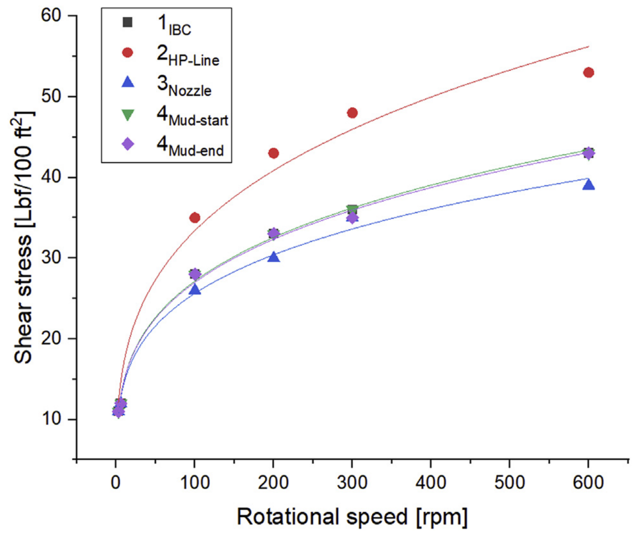

Figure 6. Rheology and Power Law fit of the sepiolite drilling and jetting fluid measured directly before and after testing (all values, except for 3_{Nozzle}, are an average from two test runs).

Unlike the sepiolite fluid, the xanthan gum fluid showed a strong degradation after the high pressure pumping as the yield point decreased from 22 to 16 Lbf/100 ft^2 and the 3 rpm value was reduced from 11 to 4 Lbf/100 ft^2 after cooling to ambient (Table 11). The fluid which passed through the nozzle was degraded even further as it retained almost no viscosity, the 3 rpm shear rate was reduced from 11 Lbf/100 ft^2 in the IBC to 1 Lbf/100 ft^2 after exiting the jetting nozzle even after the fluid was cooled to ambient. When measured near to the actual test temperature (Table 10), the viscosity reduction was even more pronounced. Generally, the xanthan gum fluid samples showed excellent fits with the Bingham model as well as the Power Law model.

As the jetted fluid mixed with the drilling fluid, the viscosity of the drilling mud sample after the 10 min test run was therefore reduced as well (600 rpm value dropped from 43 to 34 Lbf/100 ft^2 while the 3rpm value was reduced to 9 Lbf/100 ft^2 from 11 Lbf/100 ft^2 initially). This fluid therefore possesses a reduced hole cleaning ability as the jetting fluid exhibited little to none carrying capacity.

While the passage through the high pressure tubing decreased fluid viscosity, the jetting through the nozzle thoroughly degraded the fluid. This effect was visually noticeable as the jetted sample was optically more similar to samples aged for 16 h at temperatures above 100 °C.

Previous tests with xanthan gum and sepiolite drilling fluids had shown that after 16 h of hot roll, the high shear rate values (300 and 600 rpm) of the sepiolite fluid showed a slight decrease starting at 80°C, while for the xanthan gum fluid this decrease started at 120 °C (Echt and Plank, 2019). Due to the short testing time here (10 min) combined with the observation that a decrease of the high shear rate values of sepiolite was not observed, which should have occurred before xanthan gum if the reason was thermal degradation, it is most likely that the strong reduction in xanthan gum fluid viscosity was solely mechanical. The extreme

Table 8. Comparison of the model parameters for the sepiolite drilling and jetting fluid measured directly before and after testing (all values, except for 3_{Nozzle}, are an average from two test runs).

Sampling point	Temp.	Eqs. (1) and (2)		Bingham model			Power Law		
		YP (Lbf/100 ft^2)	PV (cP)	YP_M (Lbf/100 ft^2)	PV_M (cP*s)	R^2	K (Lbf/100 $ft^2{*}s^n$)	n	R^2
1_{IBC}	24 °C	29	7	16.7	24.8	0.75	8.1	0.26	0.997
$2_{HP\text{-}Line}$	47 °C	43	5	19.8	33.1	0.68	8.8	0.29	0.977
3_{Nozzle}	48 °C	31	4	16.2	22.0	0.74	8.2	0.25	0.993
$4_{Mud\text{-}start}$	24 °C	29	7	16.7	24.8	0.75	8.1	0.26	0.997
$4_{Mud\text{-}End}$	38 °C	27	8	16.7	24.6	0.76	8.1	0.26	0.995

Table 9. Comparison of the model parameters of the sepiolite drilling and jetting fluid measured after the collected samples were cooled to 22 °C (all values, except for 3_{Nozzle}, are an average from two test runs).

Sampling point	Eqs. (1) and (2)		Bingham model			Power Law		
	YP (Lbf/100 ft^2)	PV (cP)	YP_M (Lbf/100 ft^2)	PV_M (cP*s)	R^2	K (Lbf/100 ft^{2}*s^n)	n	R^2
1_{IBC}	31	6	16.8	24.9	0.75	8.1	0.26	0.996
$2_{HP\text{-}Line}$	44	5	22.4	31.6	0.65	10.8	0.26	0.978
3_{Nozzle}	29	6	16.4	23.3	0.76	8.1	0.25	0.997
$4_{Mud\text{-}start}$	30	7	16.9	25.7	0.76	8.0	0.27	0.997
$4_{Mud\text{-}End}$	29	7	16.9	24.8	0.74	8.2	0.26	0.995

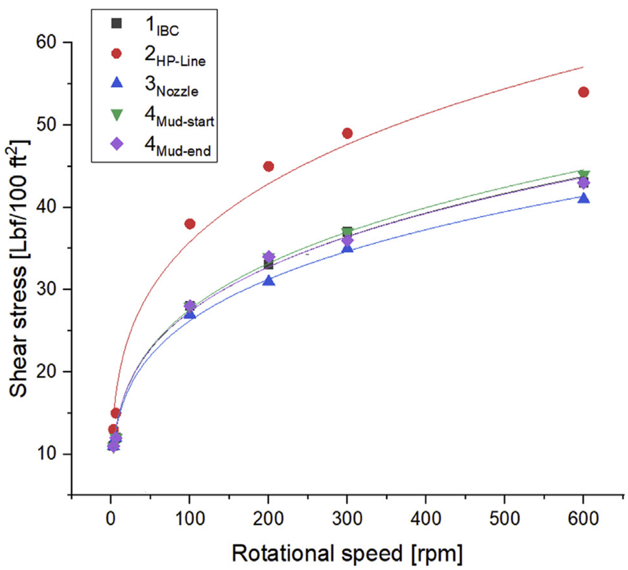

Figure 7. Rheology and Power Law fit of the sepiolite drilling and jetting fluid measured after the collected samples were cooled to 22 °C (all values, except for 3_{Nozzle}, are an average from two test runs).

loss in viscosity was due the very high shear rates during high pressure pumping and jetting.

4. Conclusion

Full scale drilling experiments using an 8 ½ inch drill bit prototype combining rotary drilling with high pressure fluid jetting and using two different drilling fluids as well as water as a reference were carried out. The novel drill bit showed an increased ROP in granite of over 70 % using either water or sepiolite compared to conventional drilling without jetting. As carrying capacity of the fluid plays little role in these granite cores due to the low height, the results for sepiolite were excellent as they showed that the sepiolite drilling did not impede the jetting process despite of the much higher viscosity compared to water.

With the conventional drill bit, similar drilling performances were achieved for sepiolite and water. However, the ROP with the xanthan gum system was slightly lower, presumably due to a lower flowability of the xanthan gum system compared with sepiolite fluid as it the xanthan gum fluid cannot flow into the induced cracks in the granite as well thus pressing the cuttings against the granite and reducing cutting removal efficiency.

The sepiolite drilling fluid maintained its excellent properties despite the very high shear rates occurring during high pressure pumping and jetting. This is highly advantageous for the current application as it means that the fluid can be used continuously over long periods of time without the need for replenishment as retains its excellent rheological properties, high yield point and high low shear rate viscosity combined with low plastic viscosity and high flow ability. Regarding the fact that in various geothermal drilling operations water cannot be used as drilling fluid due to limitations concerning bore hole stability, carrying capacity and others, the sepiolite drilling fluid poses a highly interesting and promising alternative.

Table 10. Comparison of the model parameters of the xanthan gum drilling and jetting fluid measured directly before and after testing.

Sampling point	Temp.	Eqs. (1) and (2)		Bingham model			Power Law		
		YP (Lbf/100 ft^2)	PV (cP)	YP_M (Lbf/100 ft^2)	PV_M (cP*s)	R^2	K (Lbf/100 ft^{2}*s^n)	n	R^2
1_{IBC}	20 °C	21	11	14.1	25.0	0.94	6.5	0.28	0.950
$2_{HP\text{-}Line}$	59 °C	14	6	5.6	18.7	0.83	1.7	0.43	0.994
3_{Nozzle}	55 °C	7	4	1.8	11.5	0.94	0.3	0.60	0.985
$4_{Mud\text{-}start}$	20 °C	21	11	14.2	24.8	0.94	6.6	0.28	0.951
$4_{Mud\text{-}End}$	26 °C	19	7	11.3	19.1	0.92	5.4	0.28	0.953

Table 11. Comparison of the model parameters of the xanthan gum drilling and jetting fluid measured after the collected samples were cooled to 22 °C.

Sampling point	Eqs. (1) and (2)		Bingham model			Power Law		
	YP (Lbf/100 ft^2)	PV (cP)	YP_M (Lbf/100 ft^2)	PV_M (cP*s)	R^2	K (Lbf/100 ft^{2}*s^n)	n	R^2
1_{IBC}	22	10	13.8	24.6	0.93	6.3	0.29	0.958
$2_{HP\text{-}Line}$	16	7	8.3	19.8	0.82	3.1	0.36	0.997
3_{Nozzle}	10	5	3.4	14.8	0.88	0.9	0.49	0.992
$4_{Mud\text{-}start}$	21	11	14.0	25.0	0.94	6.4	0.29	0.942
$4_{Mud\text{-}End}$	20	7	11.3	20.0	0.93	5.1	0.29	0.945

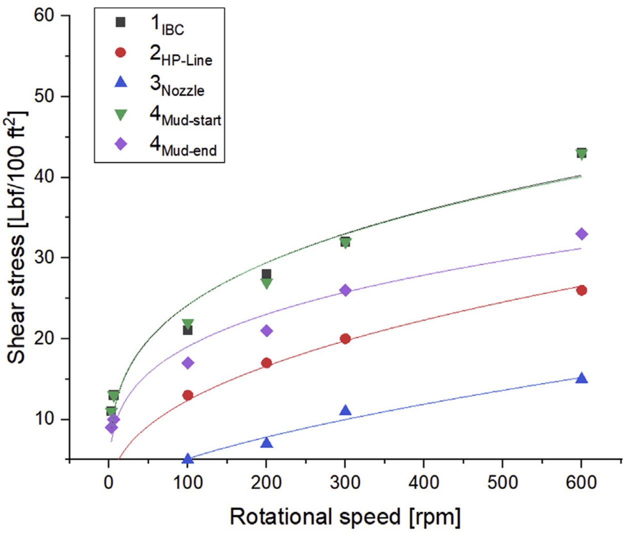

Figure 8. Rheology and Power Law fit of the xanthan gum drilling and jetting fluid measured directly before and after testing.

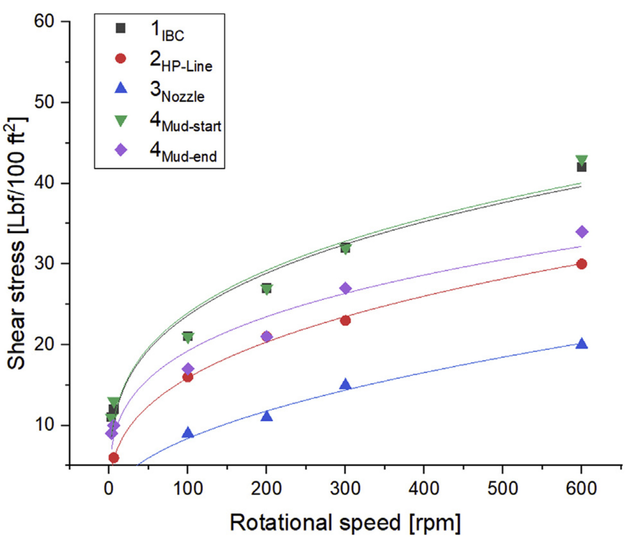

Figure 9. Rheology and Power Law fit of the xanthan gum drilling and jetting fluid measured after the collected samples were cooled to 22 °C.

The xanthan gum fluid was degraded significantly through by the high shear rates occurring during pumping and jetting as the low shear rate viscosity was reduced from 11 Lbf/100 ft^2 in the pristine fluid to 1 Lbf/100 ft^2 after exiting the jetting nozzle. The resulting xanthan gum fluid possesses little to none carrying capacity and subsequently would show a limited hole cleaning ability in the field for applications in combination with the high pressure fluid jet assisted rotary drilling system.

Declarations

Author contribution statement

Timon Echt: Conceived and designed the experiments; Performed the experiments; Analyzed and interpreted the data; Contributed reagents, materials, analysis tools or data; Wrote the paper.

Thomas Stoxreiter: Conceived and designed the experiments; Performed the experiments; Analyzed and interpreted the data; Contributed reagents, materials, analysis tools or data; Wrote the paper.

Johann Plank: Conceived and designed the experiments; Analyzed and interpreted the data; Contributed reagents, materials, analysis tools or data; Wrote the paper.

Funding statement

The work in this study was carried out within the ThermoDrill project which has received funding from the European Union's Horizon 2020 research and innovation programme under grant agreement No. 641202.

Competing interest statement

The authors declare no conflict of interest.

Additional information

No additional information is available for this paper.

Acknowledgements

The authors would like to thank Alexander Buchner of Sirius for the preparation of the xanthan gum drilling fluid and all of the involved ThermoDrill partners for their support as well as Laurent Gerbaud and his team of the drilling laboratory in Pau for their help and assistance during the testing. We are also very grateful for the support by the team of the technical centre of URACA GmbH & Co. KG.

References

Altun, G., Osqouei, A.E., Ozyurtkan, M.H., Serpen, U., 2015. Sepiolite Based Muds as an Alternate Drilling Fluid for Hot Environments. Presented at the World Geothermal Congress, Melbourne, Australia.
API, 2004. RP 13B-1: Recommended Practice for Field Testing Water-Based Drilling Fluids, fourth ed. American Petroleum Institute: Washington D.C., USA.
Becker, T.E., Azar, J.J., Okrajni, S.S., 1991. Correlations of mud rheological properties with cuttings-transport performance in directional drilling. SPE Drill. Eng. 6 (1).
Caenn, R., Chillingar, G.V., 1996. Drilling fluids: state of the art. J. Petrol. Sci. Eng. 14, 221–230.
Diethart-Jauk, E., Gegenhuber, N., 2018. Shear weakening for different lithologies observed at different saturation stages. J. Appl. Geophys. 148, 107–114.
Echt, T., Plank, J., 2019. An improved test protocol for high temperature carrying capacity of drilling fluids exemplified on a sepiolite mud. J. Nat. Gas Sci. Eng. 70, 102964.
Garnier, A.J., van Lingen, N.,H., 1958. Phenomena affecting drilling rates at depth. In: SPE-1097-G, Presented at the 33rd Annual Fall Meeting of SPE. Houston, USA.
IARC (International Agency for Research on Cancer), 1997. IARC Monographs on the Evaluation of Carcinogenic Risks to Humans, 68. Summary of Data Reported and Evaluation Sepiolite.
Kolle, J.J., 1987. Jet kerfing parameters for confined rock. In: Presented at the Fourth U.S. Water Jet Conference. Berkeley, USA.
Mansell, J., Haughs, J., 2018. High shear rheology and its direct impact on the rate of penetration. Oil Gas Eur. Mag. 1.
Maurer, W.C., Heilhecker, J.K., Love, W.W., 1973. High-pressure drilling. J. Petrol. Technol. 25 (7), 851–859.
Reichman, J.M., 1977. Research and Development of a High-Pressure Waterjet Coring Device for Geothermal Exploration and Drilling. Report for U.S. Department of Energy.
Robinson, L., Morgan, M., 2004. Effect of hole cleaning on drilling rate and performance. In: AADE-04-DF-HO-42, Presented at the AADE 2004 Drilling Fluids Conference. Houston, USA.
Stoxreiter, T., Martin, A., Teza, D., Galler, R., 2018. Hard rock cutting with high pressure jets in various ambient pressure regimes. Int. J. Rock Mech. Min. Sci. 108, 179–188.
Stoxreiter, T., Portwood, G., Gerbaud, L., Seibel, O., Essl, S., Plank, J., Hofstätter, H., 2019. Full-scale experimental investigation of the performance of a jet-assisted rotary drilling system in crystalline rock. Int. J. Rock Mech. Min. Sci. 115, 87–98.
Veenhuizen, S.D., O'Hanlon, T.A., Kelley, D.P., Duda, J.A., Aslakson, J.K., 1996. Ultra-high pressure down hole pump for jet-assisted drilling. In: SPE-35111-MS, Presented at the SPE/IADC Drilling Conference. New Orleans, USA.
Warren, T.M., Smith, M.B., 1985. Bottomhole stress factors affecting drilling rate at depth. J. Petrol. Technol. 37, 1523–1533.
Wise, W., Gusler, W., Hansen, N., Teutsch, B., Thomas, D., 2010. HP/HT well: fluid selection, planning and lessons learned. In: AADE Paper AADE-10-DF-HO-38, Presented at the AADE Fluids Conference and Exhibition. Houston, USA.
Zilch, H.E., Otto, M.J., Pye, D.S., 1991. The evolution of geothermal drilling fluid in the imperial valley. In: SPE 21786, Presented at the SPE Western Regional Meeting. Long Beach, USA.